Optical pattern selection by a lateral wave-front shift

P. L. Ramazza, S. Boccaletti, A. Giaquinta,* E. Pampaloni, S. Soria,† and F. T. Arecchi‡
Istituto Nazionale di Ottica, 50125 Firenze, Italy

(Received 2 February 1996)

We report experimental evidence of a series of transitions over different classes of two-dimensional patterns (hexagons, horizontal rolls, vertical rolls, zigzags) observed in a nonlinear optical system in which nonlocal interactions have been introduced by a lateral wave-front shift. At variance with similar scenarios of transitions observed in fluid dynamics, here the pattern selection is operated by the nonlocality mechanism, and a simple theoretical analysis yields predictions in good agreement with the experiment. [S1050-2947(96)10509-6]

PACS number(s): 42.65.−k, 03.40.Kf, 42.60.Jf, 89.90.+n

Pattern formation in spatially extended systems driven out of thermodynamical equilibrium is a rather ubiquitous phenomenon in nature [1–3]. Selection of length scales and shape of the structures that form can be due to several agents, as the symmetries (either intrinsic [4,5] or induced by boundary conditions [6–8]), or the rate of energy feeding into the system (the so-called ''pump parameter'') [9,10], or the local interactions within the system [11,13], or nonlocal interactions [14–16].

In this paper we give experimental evidence of a chain of transitions in two-dimensional patterns (hexagons→horizontal rolls→vertical rolls→zigzags) observed for a monotonic increase of a lateral wave-front shift in the feedback loop of a nonlinear optical device. The variation of this nonlocality parameter is completely responsible for the observed transitions. This point constitutes the main difference between the instabilities reported here and similar ones observed in fluid dynamics systems [9,10].

The experimental system consists of a liquid-crystal light valve (LCLV) illuminated by a spatially uniform laser beam and inserted in an optical feed-back loop [15]. The LCLV is a sandwich formed by a nematic liquid crystal layer, a mirror and a photoconductor, with an applied alternating current (ac) supply voltage. This configuration induces in the liquid-crystal layer a refractive index variation Δn that for certain ranges of the experimental parameters [17] is proportional to the optical intensity on the photoconductor (optical Kerr effect).

Pattern formation in a Kerr-like medium with various kinds of optical feedback loops has been predicted [15,18] and observed [15,19–21]. When the feedback loop consists of a free propagation path of length L, pattern formation arises by the interplay of the Kerr effect with the space dependences due to diffraction of the optical wave and diffusion of the refractive index perturbations. Furthermore, inclusion of a nonlocal interaction by means of transverse displacement of the optical wave front by an amount Δx within the feedback loop (along a given direction x transverse to that of the wave-front propagation) induces a new class of pattern forming instabilities. Instabilities of this kind were reported in Refs. [16], [22], and [23]; however these observations were limited either to small Δx for which only rolls appear [16,23], or to one transverse dimension [22]. Here we show how in two dimensions different symmetries go sequentially above threshold by a smooth variation of Δx over a wide range.

The experimental results here reported are obtained for fixed wavelength (λ=514 nm) and polarization (parallel to the liquid-crystal director) of the incoming beam, amplitude, and frequency of the voltage applied to the LCLV (V_0=12.5 V rms, ν=4 kHz and free propagation length (L=26 cm). Figure 1 shows the sequence of patterns observed in the near field (above) and in the far field (spatial Fourier transform of the near field) (below) at a fixed value of input intensity I_0=72 μW/cm^2 for increasing Δx.

At $\Delta x=0$ [Fig. 1(a)] stationary hexagons are observed. For $20<\Delta x<170$ μm [Fig. 1(b)], hexagons lose stability and are substituted by stationary rolls with length scale independent of Δx and oriented along Δx. At $\Delta x=180$ μm [Fig. 1(c)] a cross-roll pattern formed by the coexistence of horizontal and vertical rolls emerges. Vertical rolls prevail over horizontal ones for $200<\Delta x<260$ μm [Fig. 1(d)], and display a pitch that increases for increasing Δx. These rolls drift in time in the Δx direction with a velocity that is a decreasing function of Δx. For $\Delta x\simeq 270$ μm transverse distortions of vertical rolls begin to form, ending up with zigzag generation [Fig. 1(e)].

Similar scenarios (an initially stationary roll pattern evolving toward cross roll and zigzag) occur in fluid convection as the rate of energy feeding into the system increases [9,10]. These secondary instabilities were theoretically modeled, either starting from the complete set of partial differential equations describing the phenomenon [9], or relying on simplified equations (''amplitude equations'') derived from the original equations by perturbative techniques [24–26]. The same amplitude equations are valid also for the description of large section laser dynamics [27].

Here, instead, the pump parameter is kept at a fixed value, and most of the features of the observed transitions are accounted for by a linear stability analysis of the equations governing the phenomenon. The equation for the space-time evolution of the refraction index $n(x,y,t)[(x,y)$ is the plane

*Also at Dip. di Ingegneria Informatica e dell'Automazione, Università di Firenze, Firenze, Italy.

†Permanent address: Department E.C.M., Universitat de Barcelona, Spain.

‡Also at Dip. di Fisica, Università di Firenze, Firenze, Italy.

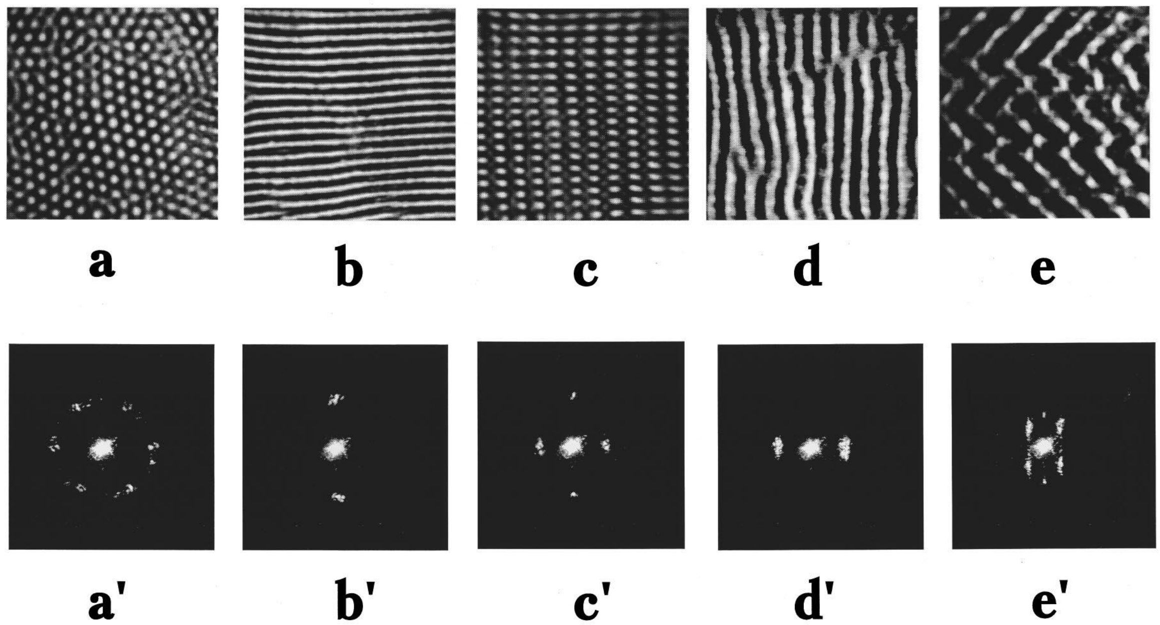

FIG. 1. Near field (above) and far field (below) patterns observed for fixed input intensity ($I_0=72$ μW/cm^2). a,a': $\Delta x=0$; b,b': $\Delta x=50$ μm; c,c': $\Delta x=180$ μm; d,d': $\Delta x=220$ μm; $e,e'=400$ μm.

transverse to the direction z of wave-front propagation] for the liquid crystal layer [15,18] reads

$$\tau\frac{\partial n(x,y,t)}{\partial t}=-n(x,y,t)+l_d^2\nabla_\perp^2 n(x,y,t)+\alpha I_{\rm fb}(x+\Delta x,y,t), \qquad (1)$$

where $\tau\simeq 100$ ms, l_d are, respectively, the response time and the diffusion length of the liquid crystal, $\nabla_\perp^2$ is the Laplacian operator in the (x,y) plane, $I_{\rm fb}(x+\Delta x,y,t)$ is the feedback intensity displaced by Δx along x, and α is a coefficient giving the strength and the sign of the Kerr nonlinearity ($\alpha>0$ for focusing media, $\alpha<0$ for defocusing media).

The Kerr approximation here adopted for the description of the LCLV is valid under two basic conditions [17]: first, the supply voltage V_0 must be larger than a threshold $V_{\rm th}$, below which the orientation of the liquid-crystal molecules remain in its initial state; second, the input intensity I_0 must be much smaller than the value $I_{\rm sat}$, at which saturation of the molecules orientation occurs. For our LCLV we measured $V_{\rm th}\simeq 3$ V rms and $I_{\rm sat}\simeq 1$ mW/cm^2, so that the Kerr approximation is valid in all the cases here considered.

With the spatial Fourier transform $(x,y)\rightarrow(q_x,q_y)\equiv\vec{q}$, Eq. (1) becomes an ordinary temporal differential equation in the Fourier space $(q_x,q_y)\equiv\vec{q}$ for the component $n_{\vec{q}}(t)$. Linear stability analysis of such an equation gives for a perturbation of spatial frequency $\vec{q}$ a complex eigenvalue $\lambda_{\vec{q}}+i\omega_{\vec{q}}$ of the form

$$\tau\lambda_{\vec{q}}=-1-l_d^2q^2+2\alpha I_0\sin\left(\frac{q^2L}{2k_0}\right)\cos(q\Delta x\cos\varphi), \qquad (2a)$$

$$\tau\omega_{\vec{q}}=2\alpha I_0\sin\left(\frac{q^2L}{2k_0}\right)\sin(q\Delta x\cos\varphi), \qquad (2b)$$

where $k_0\equiv 2\pi/\lambda$ is the optical wave number, q is the modulus of $\vec{q}$, and φ is the angle between $\vec{q}$ and $\Delta\vec{x}$. The term in $\sin(q^2L/2k_0)$ arises from the propagative nature of the optical feedback loop [18]. We recall that in the present case $\alpha<0$ since LCLV acts as a self-defocusing medium.

By differentiating the above expressions with respect to q and φ, we find the values (q,φ) for which the growth rate $\lambda_{\vec{q}}$ has a local maximum, corresponding to the most unstable modes, which are selected by the system when driven slightly above threshold. It turns out that, for $\Delta x\neq 0$, the most unstable modes are those for which

$$\varphi=\begin{cases}\pm\dfrac{\pi}{2},\ q\simeq\sqrt{3\pi k_0/L} & \text{horizontal rolls,} \quad (3a)\\ 0,\pi,\ q=q(\Delta x) & \text{vertical rolls,} \quad (3b)\\ \pm\arccos\left[\dfrac{\pi}{q\Delta x}\right],\ q\simeq\sqrt{\pi k_0/L} & \text{oblique rolls.} \quad (3c)\end{cases}$$

In writing the expressions for the unstable wave numbers in the cases of horizontal and oblique rolls we have assumed that diffraction is dominating over diffusion in determining the length scale of the patterns [28]. This is justified by the fact that the diffusion length of the LCLV is $l_d\simeq 40$ μm, so that $l_d^2k_0/L\simeq 0.1$.

Equation (3c) predicts only that for some Δx ranges two sets of oblique rolls are linearly unstable, but does not provide information on the actual pattern. This prediction is

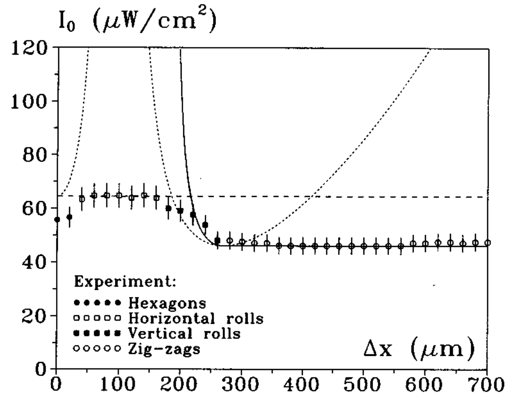

FIG. 2. Marginal stability curves ($\lambda_{\vec{q}}=0$) for horizontal rolls (dashed line), vertical rolls (dotted lines), and zigzags (solid line), and experimental values of the excitation thresholds for hexagons, horizontal rolls, vertical rolls, and zigzag pattern. The theoretical curves are evaluated for $l_d=40$ μm, $\alpha=-0.0134$ cm^2/μW (see text for definitions).

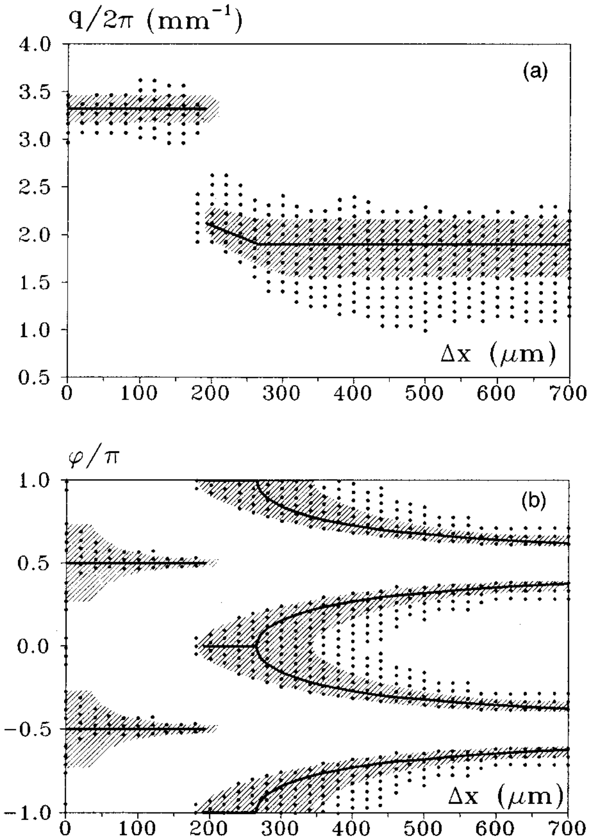

FIG. 3. Excited values of q (a) and φ (b) vs Δx, for $I_0=72$ μW/cm^2. Experiment: the dotted regions represent the bandwidth size for each Δx. Theory: the continuous lines are the modes of maximum growth rate and the shadowed regions represent modes having a relative growth rate that differs from the maximum one by less than 0.3, for the same parameters as in Fig. 2.

compatible with situations in which only one of the two sets of rolls appears, or the two sets coexist with a given phase relation. Investigating the stability properties of these various patterns would require nonlinear analysis around Eq. (3c), a task that is beyond the aims of the present work. For the parameters here selected, however, the two sets of oblique rolls have always been observed to organize in zigzag patterns as the one shown in Fig. 1(e).

In Fig. 2 we report the marginal stability curves ($\lambda_{\vec{q}}=0$) in the (Δx,I_0) plane for the Eqs. (3a)–(3c), together with the experimental instability thresholds. The theoretical curves are in fair agreement with the experimental values for a choice of the LCLV parameters $l_d=40$ μm, $\alpha=-0.0134$ cm^2/μW. The only quantitative discrepancy between theory and experiments is observed for $\Delta x\simeq 0$, since for $\Delta x=0$ the solution at threshold is the hexagonal pattern that cannot be accounted for by the linear stability analysis [28].

To test how far we can rely on the results of the linear stability analysis we compare the width of the excited q and φ bands measured for various Δx at $I_0=72$ μW/cm^2 with their theoretical counterparts. The result of these procedures are reported in Fig. 3. For each Δx, the stationary situation in which the measurements were done was reached by starting from I_0 below threshold, and gradually increasing the intensity beyond the corresponding threshold value (reported in Fig. 2) up to $I_0=72$ μW/cm^2. This procedure discriminates which of the patterns of Fig. 1 arises directly from the primary bifurcations and which pattern arises rather from secondary bifurcations. In this way we verified that the patterns here reported arise from primary bifurcations, with the exception of cross rolls, this last one being due to the superposition of horizontal and vertical rolls with different thresholds. Further secondary bifurcations leading to the appearance of more complex space-time structures are observed for values of I_0 well above 72 μW/cm^2.

The width of the bands reported in Fig. 3 is not constant, because the offset above threshold depends on Δx. The theoretical bands are calculated by assuming that, for each fixed Δx, all the wave vectors with a growth rate different by less than a faction p from its maximum are excited. Figure 3 corresponds to $p=0.3$.

In the case of the vertical rolls, we have performed a measurement of the average drift velocity v_d, and for the whole range of Δx [and corresponding q values (see Fig. 3)], where these rolls occur, v_d is confined in the interval 10 to 100 μ/s. On the other hand, from Eq. (2b) we evaluate, for $\cos\varphi=1$

$$v_d\equiv\frac{\omega}{q}=\frac{2\alpha I_0\sin\left(\frac{q^2L}{2k_0}\right)\sin(q\Delta x)}{q\tau}. \quad (4)$$

Introducing the numerical values, Eq. (4) yields values of v_d in agreement within 20% with the ones measured in the experiment. The agreement between theory and experiments confirms that the most relevant features of the observed scenario are explained by linear stability arguments.

This work was partly supported by EEC Contract Nos. CI1*CT93-0331 and CHRX-CT93-0107.

[1] J. D. Murray, *Mathematical Biology* (Springer-Verlag, Berlin, 1989).
[2] M. Cross and P. C. Hohenberg, Rev. Mod. Phys. **65**, 851 (1993).
[3] F. T. Arecchi, Nuovo Cimento A **107**, 1111 (1994); Chaos Solitons Fractals **4** (8/9), (1994) special issue on Nonlinear Optical Structures, Patterns, Chaos.
[4] S. Ciliberto, E. Pampaloni, and C. Perez-Garcia, Phys. Rev. Lett. **61**, 1198 (1988).
[5] A. B. Ezerzkii, P. I. Korotin, and M. I. Rabinovich, JETP Lett. **41**, 157 (1985).
[6] F. T. Arecchi, G. Giacomelli, P. L. Ramazza, and S. Residori, Phys. Rev. Lett. **65**, 2531 (1990).
[7] E. J. D'Angelo, E. Izaguirre, G. B. Mindlin, G. Huyet, L. Gil, and J. R. Tredicce, Phys. Rev. Lett. **68**, 3702 (1992).
[8] C. W. Meyer, G. Ahlers, and D. S. Cannell, Phys. Rev. A **44**, 2514 (1991).
[9] F. H. Busse and J. A. Whitehead, J. Fluid Mech. **47**, 305 (1971).
[10] A. Joets and R. Ribotta, J. Phys. (Paris) **47**, 595 (1986).
[11] V. Castets, E. Dulos, J. Boissonade, and P. De Kepper, Phys. Rev. Lett. **64**, 2953 (1990).
[12] F. T. Arecchi, S. Boccaletti, P. L. Ramazza, and S. Residori, Phys. Rev. Lett. **70**, 2277 (1993).
[13] M. Ohgiwari, M. Matsushita, and T. Matsuyama, J. Phys. Soc. Jpn. **61**, 816 (1992).
[14] E. D. Siggia and A. Zippelius, Phys. Rev. Lett. **47**, 835 (1991).
[15] S. A. Akhmanov, M. A. Vorontsov, and V. Yu. Ivanov, JETP Lett. **47**, 707 (1988).
[16] A. Petrossian, L. Dambly, and G. Grynberg, Europhys. Lett. **29**, 209 (1995).
[17] R. Neubecker, G. L. Oppo, and T. Tschudi, Phys. Rev. A **52**, 791 (1995).
[18] W. J. Firth, J. Mod. Opt. **37**, 151 (1990); G. D'Alessandro and W. J. Firth, Phys. Rev. Lett. **66**, 2597 (1991).
[19] R. Macdonald and H. J. Eichler, Opt. Commun. **89**, 289 (1992).
[20] S. A. Akhmanov, M. A. Vorontsov, V. Yu. Ivanov, A. V. Larichev, and N. I. Zheleznykh, J. Opt. Soc. Am. B **9**, 78 (1992).
[21] E. Pampaloni, S. Residori, and F. T. Arecchi, Europhys. Lett. **24**, 647 (1993); E. Pampoloni, P. L. Ramazza, S. Residori, and F. T. Arecchi, *ibid.* **25**, 587 (1994); Phys. Rev. Lett. **74**, 258 (1995); P. L. Ramazza, S. Residori, E. Pampaloni, and A. V. Larichev, Phys. Rev. A **53**, 400 (1996).
[22] P. L. Ramazza, P. Bigazzi, E. Pampaloni, S. Residori, and F. T. Arecchi, Phys. Rev. E **52**, 5524 (1995).
[23] R. Macdonald and H. Danlewski, Opt. Lett. **20**, 441 (1995).
[24] H. S. Greenside and M. C. Cross, Phys. Rev. A **31**, 2492 (1985).
[25] M. Kaiser and W. Pesch, Phys. Rev. E **48**, 4510 (1993).
[26] Q. Feng, W. Pesch, and L. Kramer, Phys. Rev. A **45**, 7242 (1992).
[27] J. Lega, J. V. Moloney, and A. C. Newell, Physica D **83**, 478 (1995).
[28] G. D'Alessandro and W. J. Firth, Phys. Rev. A **46**, 537 (1992).